The Journal of Veterinary Medical Science

FULL PAPER

Internal Medicine

Sorafenib inhibits tumor cell growth and angiogenesis in canine transitional cell carcinoma

Shohei YOKOTA[1)], Tomohiro YONEZAWA[1)], Yasuyuki MOMOI[1)] and Shingo MAEDA[1)]*

[1)]Department of Veterinary Clinical Pathobiology, Graduate School of Agricultural and Life Sciences, The University of Tokyo, Tokyo, Japan

J. Vet. Med. Sci.
84(5): 666–674, 2022
doi: 10.1292/jvms.21-0478

Received: 3 September 2021
Accepted: 22 March 2022
Advanced Epub:
5 April 2022

ABSTRACT. Canine transitional cell carcinoma (cTCC) is the most common naturally occurring bladder cancer and accounts for 1–2% of canine tumors. The prognosis is poor due to the high rate of invasiveness and metastasis at diagnosis. Sorafenib is a multi-kinase inhibitor that targets rapidly accelerated fibrosarcoma (RAF), vascular endothelial growth factor receptor (VEGFR)-1, VEGFR-2, VEGFR-3, platelet-derived growth factor receptor-β (PDGFR-β), and KIT. In previous studies, a somatic mutation of B-rapidly accelerated fibrosarcoma (BRAF) and expressions of VEGFR-2 and PDGFR-β were observed in over 80% of patients with cTCC. Therefore, in this study, we investigated the anti-tumor effects of sorafenib on cTCC. Five cTCC cell lines were used in the *in vitro* experiments. All five cTCC cell lines expressed VEGFR-2 and PDGFR-β and sorafenib showed growth inhibitory effect on cTCC cell lines. Cell cycle arrest at the G0/G1 phase and subsequent apoptosis were observed following sorafenib treatment. In the *in vivo* experiments, cTCC (Sora) cells were subcutaneously injected into nude mice. Mice were orally administered with sorafenib (30 mg/kg daily) for 14 days. Sorafenib inhibited tumor growth compared to vehicle control. The necrotic area in the tumor tissues was increased in the sorafenib-treated group. Sorafenib also inhibited angiogenesis in the tumor microenvironment. Thus, sorafenib may be potential therapeutic agent for cTCC via its direct anti-tumor effect and inhibition of angiogenesis.

KEYWORDS: angiogenesis, dog, sorafenib, transitional cell carcinoma, vascular endothelial growth factor receptor-2

Canine transitional cell carcinoma (cTCC), also known as urothelial carcinoma, is the most common naturally occurring bladder cancer in dogs, comprising 1–2% of all canine tumors and approximately 20,000 new cases expected each year in the United States of America (USA) [9, 16]. Due to its nonspecific clinical signs (hematuria, stranguria, and pollakiuria), early detection of cTCC is often difficult. At the time of diagnosis, tumor cells invade the muscle layers of the bladder in many cases, and 20% of cTCCs display progression with invasion to neighboring organs and present with distant metastasis [1, 16]. Current treatments for cTCC include surgery, radiation, and chemotherapy, but the majority of cTCC develops in the trigone region of the bladder, which makes radical surgery difficult. Chemotherapeutic regimens including cisplatin, carboplatin, vinblastine, mitoxantrone, and gemcitabine are the mainstay in the treatment of cTCC, and non-steroidal anti-inflammatory drugs enhance their effectiveness when treated in combination [9, 16–18, 23, 29, 32]. However, when treated with these therapies, the median survival time is less than a year and drug resistance occurs frequently; therefore, new effective therapies are needed [16].

Sorafenib is a multi-kinase inhibitor that inhibits tumor growth and angiogenesis by targeting rapidly accelerated fibrosarcoma (RAF) family of serine/threonine kinases and receptor tyrosine kinases (RTKs) including vascular endothelial growth factor receptor (VEGFR)-1, VEGFR-2, VEGFR-3, platelet-derived growth factor receptor-β (PDGFR-β), and KIT [7, 11, 31, 44]. B-rapidly accelerated fibrosarcoma (BRAF) is a member of the RAF family and plays key roles in the MAPK/ERK pathway, a signaling pathway that is involved in cell metabolism, cell cycle regulation, and cell growth. Somatic BRAF mutation, which makes the BRAF oncogene, can enhance the MAPK/ERK pathway and contribute to the occurrence and development of malignant tumors. BRAF mutation has been reported to adversely affect the prognosis of patients in the medical field [8, 37]. In a previous study, over 80% of cTCC patients had a $BRAF^{V595E}$ mutation [3, 24, 25].

*Correspondence to: Maeda, S.: amaeda@g.ecc.u-tokyo.ac.jp, Department of Veterinary Clinical Pathobiology, Graduate School of Agricultural and Life Sciences, The University of Tokyo, 1-1-1 Yayoi, Bunkyo-ku, Tokyo 113-8657, Japan
(Supplementary material: refer to PMC https://www.ncbi.nlm.nih.gov/pmc/journals/2350/)

RTKs are a subclass of tyrosine kinases that mediate cell communication and biological functions, including cell proliferation, differentiation, angiogenesis, and migration. RTK expression contributes to tumor progression and is positively correlated with poor outcomes [13, 27, 28, 30, 33, 38]. In a previous study, the expression of VEGFR-2 and PDGFR-β was observed in all cTCC patients [35]. Among RTKs, VEGFR-2 is considered a highly active receptor that contributes to tumor progression [43].

In a previous study, sorafenib treatment showed a growth inhibitory effect on human colon cancer with BRAF mutation [40]. Furthermore, in human hepatocellular carcinoma patients, VEGFR-2 and PDGFR-β expression were identified, and sorafenib increased the survival rate by 44% [2, 5, 10, 12]. VEGFR-2 expression has also been observed in 50% to 80% of human bladder cancers, and sorafenib has shown a growth inhibitory effect on human bladder cancer cell lines [19, 21, 36]. Regarding cTCC, sorafenib showed anti-tumor effect on cTCC cell lines with BRAF mutation and a case report showed that sorafenib was effective on cTCC patient which overexpressed VEGFR [14, 15]. Then, we hypothesized that sorafenib may be effective against cTCC. In the present study, we investigated the effect of sorafenib on cTCC *in vitro* and *in vivo*. We investigated the expression level of VEGFR-2 and PDGFR-β. Moreover, we examined the activity of downstream signals of RTKs and BRAF and performed cell cycle and apoptosis assays. In *in vivo* experiments, we investigated the growth inhibitory effect of sorafenib along with its effect on angiogenesis in the TME.

MATERIALS AND METHODS

Cell lines

We used five cTCC cell lines (Sora, Love, MCTCC, LCTCC, and TCCUB) [39, 41]. The $BRAF^{V595E}$ mutation was observed in all cell lines [6]. The cell lines were cultured in RPMI-1640 medium (Sigma-Aldrich, St. Louis, MO, USA) supplemented with 10% fetal bovine serum (Gibco, Carlsbad, CA, USA) and 1% penicillin-streptomycin at 37°C with 5% CO_2. All cell lines were tested for mycoplasma using the EZ-PCR Mycoplasma Test Kit (Biological Industries, Cromwell, CT, USA).

Reagents

Sorafenib used in the *in vitro* and *in vivo* experiments were purchased from Santa Cruz Biotechnology (Dallas, TX, USA) and Chem Scene (Monmouth, NJ, USA), respectively. Canine vascular endothelial growth factor (VEGF) was purchased from Kingfisher Biotech (Saint Paul, MN, USA). For western blotting, anti-PDGFR-β, anti-ERK 1/2, anti-Tyr 202/Tyr 204-phosphorylated ERK 1/2, anti-Akt, and anti-Ser 473-phosphorylated Akt antibodies were purchased from Cell Signaling Technology (Danvers, MA, USA). Anti-VEGFR-2, anti-caspase 9 (p35), and anti-β-actin antibodies were purchased from Santa Cruz Biotechnology. IRDye 680RD donkey anti-mouse, IRDye 800CW donkey anti-rabbit, and IRDye 800CW PEG Fluorescent Contrast Agent were purchased from MandS TechnoSystems Inc. (Osaka, Japan). Goat Anti-Mouse IgG Biotin Conjugate was purchased from Tokyo Chemical Industry Co., Ltd. (Tokyo, Japan). Streptavidin-HRP reagent was purchased from Dako (Santa Clara, CA, USA). For immunofluorescence, anti-cleaved caspase 3 antibody was purchased from Cell Signaling Technology, and anti-CD31 antibody was purchased from Biocare Medical (Pacheco, CA, USA). Alexa Fluor® 647 conjugated anti-rat antibody was purchased from Abcam (Cambridge, UK), and 4',6-diamidino-2-phenylindole (DAPI) was purchased from Thermo Fisher Scientific.

Cell proliferation assay

The cells were seeded in 96 well plates and incubated for 24 hr. The cells were treated with a concentration of sorafenib (2.5–20 μM) for 48 hr. After the treatment, the cells were fixed with 10% trichloroacetic acid (Wako, Osaka, Japan) at 4°C for 1 hr, washed twice with phosphate buffered saline (PBS), and stained with 0.057% sulforhodamine B (Sigma-Aldrich) at room temperature for 30 min. Following staining, the cells were washed four times with 1% acetic acid and dried completely. The protein-bound dye was dissolved in 10 mM Tris base solution, and absorbance was measured at 490 nm using a microplate reader (Bio-Rad, Hercules, CA, USA).

Western blotting

To evaluate ERK and Akt signals after treatment with sorafenib, cTCC cells seeded on 6 well plates were treated with a concentration of sorafenib (2.5–20 μM) for 1 hr followed by treatment with or without 30 ng/ml VEGF at 37°C for 15 min. Radioimmunoprecipitation assay buffer (cell signaling) containing protease inhibitor and phosphatase inhibitor cocktail tablets (Roche Diagnostics, Mannheim, Germany) were used to extract cell and tissue lysates, and total protein levels were measured using a BCA protein assay kit (Thermo Fisher Scientific). Equal amounts of samples were separated by 10% SDS polyacrylamide gel electrophoresis and transferred onto nitrocellulose membranes. After blocking with 5% skim milk in Tris-buffered saline (TBS) containing 0.1% Tween 20 at room temperature for 1 hr, the membranes were incubated with primary antibodies (VEGFR-2 1:100, PDGFR-β 1:100, p-ERK 1:300, ERK 1:300, p-Akt 1:300, Akt 1:300, caspase 9 1:300, β-actin 1:1,000) at 4°C overnight. The membranes were washed and incubated with the appropriate secondary antibodies at room temperature for 1 hr. As for anti-VEGFR-2 antibody, following incubation with primary antibody, the membrane was incubated with corresponding biotinylated secondary antibody (1:200) at room temperature for 2 hr followed by the incubation with Streptavidin-HRP conjugate (1:300) at room temperature for 1 hr. The membrane was subsequently washed and developed using chemiluminescent reagent. The proteins were visualized using ODYSSEY CLx (MandS TechnoSystems Inc.).

Cell cycle analysis

Cells seeded in 6 well plates were treated with DMSO and 10 μM and 20 μM sorafenib for 24 hr. After treatment, the cells were fixed with 70% pre-chilled ethanol for over 2 hr at 4°C. The fixed cells were washed twice with PBS and treated with RNase A (QIAGEN, Hilden, Germany) at a final concentration of 0.25 mg/ml at 37°C for 30 min to obviate staining due to RNA. Nuclei were then stained with propidium iodide (PI) (Sigma-Aldrich) at a final concentration of 50 μg/ml on ice for 30 min. The DNA content of the cells was evaluated using a FACS flow cytometer (BD Biosciences, Tokyo, Japan), and the frequency of cells in each cell cycle phase was measured.

Terminal deoxynucleotidyl transferase dUTP nick end labeling (TUNEL) staining

The cells were seeded on cover glasses, incubated for 24 hr, and then treated with DMSO or 20 μM sorafenib for 24 hr. After treatment, the cells were washed with PBS and fixed with 4% paraformaldehyde at 4°C for 25 min. Apoptosis was detected using the DeadEnd Fluorometric TUNEL System (Promega, Madison, WI, USA) according to the manufacturer's protocol. Cells treated with 1 U DNase I (Promega) were used as a positive control.

Mouse xenograft model

Male BALB/c nude mice (5–6 weeks old) were purchased from Japan SLC, Inc. (Shizuoka, Japan) and acclimated to our facilities for one week. In the cTCC subcutaneous model, 2×10^6 Sora cells were subcutaneously implanted into the left flank of each mouse. Two days later, mice were randomly divided into two groups and treated with PBS or sorafenib (30 mg/kg) daily for 14 days. Subcutaneous tumor growth was recorded as the length and width of tumors using a Vernier caliper every 2 days, and the tumor size was calculated using the formula, (length × width × height)/2. On day 16, the mice were euthanized, and the tumors were collected for histological analysis and immunofluorescence. All procedures were approved by the Animal Care and Use Committee of The University of Tokyo (authorization number: P20-116).

Histopathological analysis

Tumor tissues were isolated from the tumor-engrafted mice. Four percent paraformaldehyde-fixed, paraffin-embedded tissue blocks were prepared and cut into 4-μm sections. The sections were stained with hematoxylin and eosin and evaluated using a light microscope BZ-X810 (Keyence, Osaka, Japan). The percentage of the necrotic area in each tumor tissue was calculated using an imaging software (BZ-800 Analyzer).

Immunofluorescence

Tumor tissues were isolated from tumor-engrafted mice and frozen in OCT compound. The sections were cut into 10-μm thickness from frozen blocks using a cryostat. For immunofluorescence, the sections were fixed with ice-cold acetone at −20°C for 10 min. After blocking with 5% bovine serum albumin in TBS containing 0.1% Tween 20 at room temperature for 30 min, the sections were incubated with anti CD31 (1:500) or cleaved caspase 3 (1:300) antibodies at 4°C overnight. The sections were washed and stained with the appropriate secondary antibody at room temperature for 1 hr, followed by staining of nuclei with DAPI. The figures were analyzed using BZ-X810 (Keyence). As for CD31 staining, the CD31 positive area (μm^2) was measured at HPF at 10 views per specimen using imaging software (BZ-800 Analyzer). The average CD31-positive area in vehicle control and sorafenib treated groups were calculated respectively and the ratio to vehicle control group were shown.

Vascular in vivo imaging

For vascular *in vivo* imaging, 2×10^6 Sora cells were subcutaneously implanted into the left flank of Male BALB/c nude mice (5–6 weeks old). Thirty days later, mice were randomly divided into two groups and treated with PBS or sorafenib (30 mg/kg) daily for 14 days. Then, mice were injected intravenously with 1 nmol/100 μl of IRDye 800CW PEG Fluorescent Contrast Agent (MandS TechnoSystems Inc.). After 24 hr, the mice were euthanized and tumor tissues were collected. Fluorescence imaging at 800 nm in tumor tissues were immediately carried out using ODYSSEY CLx. The fluorescence intensity in each sample were automatically measured and the average in vehicle control and sorafenib treated groups were calculated respectively.

Statistical analysis

Student's *t*-test was used for comparisons between the two groups. Statistical significance was set at $P<0.05$. The analysis was conducted using Prism software (version 5.0.1; GraphPad Software, San Diego, CA, USA).

RESULTS

Anti-tumor effect of sorafenib on cTCC cell lines

All five cTCC cell lines expressed VEGFR-2 (Fig. 1A). PDGFR-β expression was also observed in all five cTCC cell lines (Fig. 1B). We performed a sulforhodamine B (SRB) assay to evaluate the growth inhibitory effect of sorafenib on cTCC cell lines. Sorafenib treatment for 48 hr inhibited cell growth in all cTCC cell lines (Fig. 1C). The percentage of cell death increased in sorafenib in a dose-dependent manner with an IC50 from 3.84 μM in Sora, 4.77 μM in LCTCC, 5.84 μM in Love, 7.03 μM in MCTCC, and 6.90 μM in TCCUB.

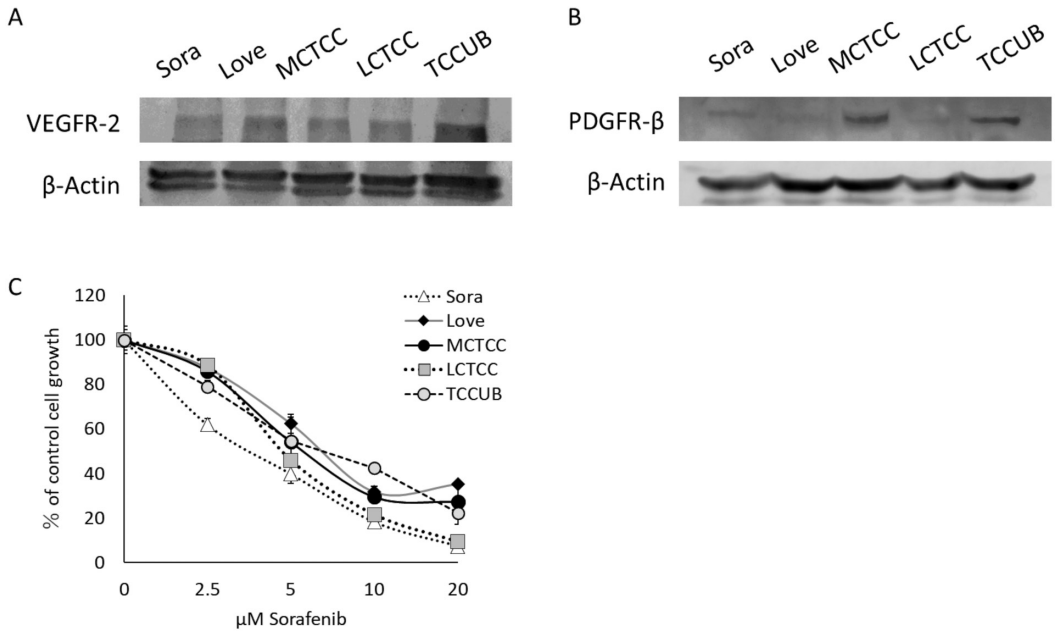

Fig. 1. Vascular endothelial growth factor receptor 2 (VEGFR-2) and platelet endothelial growth factor receptor β (PDGFR-β) expression and the effects of sorafenib on canine transitional cell carcinoma (cTCC) cell lines. (**A**) VEGFR-2 expression in cTCC cell lines was analyzed using western blotting. (**B**) PDGFR-β expression in cTCC cell lines was analyzed using western blotting. (**C**) The cytotoxicity effect of sorafenib on cTCC cell lines (Sora, Love, MCTCC, LCTCC, and TCCUB). CTCC cell lines were treated with 2.5–20 μM of sorafenib for 48 hr. The percentage of cell viability was determined by sulforhodamine B assay. Each value represents the mean ± SD.

Effects of sorafenib on signaling pathways, cell cycle, and apoptosis

We further investigated the molecular mechanism by which sorafenib inhibited the growth of cTCC cell lines. First, we performed western blotting to investigate the effect of sorafenib on the MAPK/ERK and PI3K/Akt pathways. Autophosphorylation of ERK and Akt was not observed in the unstimulated cTCC cell lines (Fig. 2A). VEGF treatment induced the phosphorylation of ERK but not Akt in all cTCC cell lines (Fig. 2B, Supplementary Fig. 1). ERK phosphorylation was strongly suppressed by the treatment with sorafenib in Sora, LCTCC, and TCCUB, while modestly suppressed in Love (Fig. 2B, 2C, Supplementary Fig. 1). On the other hand, though 2.5 to 10 μM of sorafenib suppressed ERK phosphorylation, rebound was observed at 20 μM of sorafenib in MCTCC (Supplementary Fig. 1). Next, we investigated the effects of sorafenib on the cell cycle. The results showed that sub-G1 and G0/G1 phase fractions increased, while S and G2/M phase fractions were reduced in Sora, MCTCC, and TCCUB after treatment with 10 μM of sorafenib (Fig. 2D, 2E, Supplementary Fig. 2). In Love and LCTCC, 10 μM sorafenib remarkably increased the sub-G1 fraction, and 20 μM sorafenib increased the proportion even more (Supplementary Fig. 2). We performed TUNEL staining to examine whether sorafenib induced apoptosis. TUNEL-positive cells were observed in Sora, Love, MCTCC, and TCCUB, but not in LCTCC cells (Fig. 2F, Supplementary Fig. 3).

Anti-tumor effect of sorafenib on cTCC engrafted mice

We investigated the effects of sorafenib on a xenograft mouse model. We confirmed that oral administration of sorafenib (30 mg/kg, daily) effectively inhibited tumor growth in cTCC-engrafted mice (Fig. 3A). Tumor volume and weight significantly decreased in the sorafenib-treated group relative to the control group (Fig. 3A–C). With regard to body weight, there was no significant difference between the sorafenib and control groups, and no side effects of sorafenib were observed during the treatment (Supplementary Fig. 4). We performed hematoxylin and eosin staining to investigate histological findings. The necrotic area in the tumor tissues increased in the sorafenib-treated group (Fig. 3D). The percentage of necrotic area in the control and sorafenib-treated groups was 1.78 ± 1.03% and 26.39 ± 6.91%, respectively (Fig. 3E).

Effect of sorafenib on angiogenesis and apoptosis in cTCC engrafted mice

We evaluated the vessel area in tumor tissues by vascular imaging and CD31 immunofluorescence. IRDye 800CW PEG accumulated in tumor blood vessels and was visualized by fluorescence (Fig. 4A). The fluorescence intensity in the sorafenib-treated group was lower than that in the vehicle control group (Fig. 4A–C). CD31 immunofluorescence confirmed that sorafenib inhibited angiogenesis in the tumor tissues (Fig. 4D, 4E). As for apoptosis, sorafenib increased caspase 9 expression (Fig. 4F, 4G) and the rate of cleaved caspase 3 positive cells in tumor tissues (Fig. 4H, 4I), suggesting that sorafenib induced apoptosis in tumor tissue.

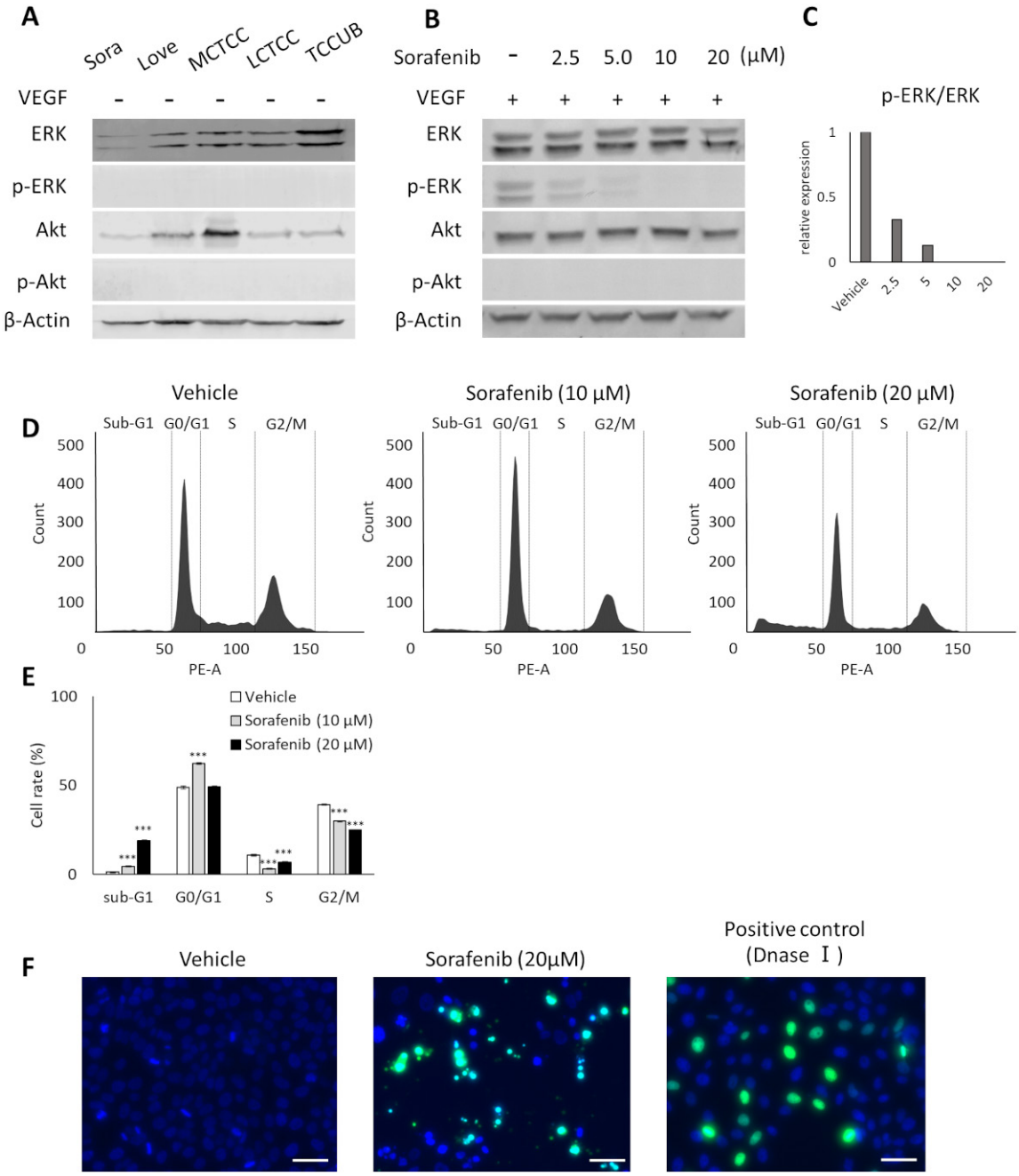

Fig. 2. Autophosphorylation of signaling pathways and the effects of sorafenib on signaling pathways, cell cycle, and apoptosis of canine transitional cell carcinoma (cTCC) cell line. (**A**) Autophosphorylation of ERK and Akt in cTCC cell lines (Sora, Love, MCTCC, LCTCC, TCCUB). (**B**) Effect of sorafenib on ERK and Akt phosphorylation in cTCC cells (Sora). The cells were treated with 2.5–20 μM of sorafenib for 1 hr, followed by treatment with 30 ng/ml vascular endothelial growth factor for 15 min. p-ERK: Tyr 202/Tyr 204-phosphorylated ERK, p-Akt: Ser 473-phosphorylated Akt. (**C**) The relative expression levels of p-ERK in cTCC cells (Sora). The Band densities of p-ERK were quantitated and normalized using ERK as corresponding control. The normalized values for each group were shown with the vehicle control as the reference. (**D**) The images of the cell cycle analysis of cTCC cells (Sora). The cells were treated with 10 μM and 20 μM of sorafenib for 24 hr, and the DNA content was analyzed by flow cytometry. (**E**) The proportion of sub-G1, G0/G1, S, and G2/M phase fraction in Sora cells after treatment with sorafenib. Each value represents the mean ± SD. (**F**) Apoptosis of cTCC cells (Sora) after treatment with sorafenib. The cells were treated with 20 μM of sorafenib for 24 hr and apoptotic cells were detected by the terminal deoxynucleotidyl transferase dUTP nick end labeling (TUNEL) methods. Green fluorescence indicates TUNEL signals, and blue indicates 4',6-diamidino-2-phenylindole (DAPI) signals. Bar=50 μm. ***P<0.001.

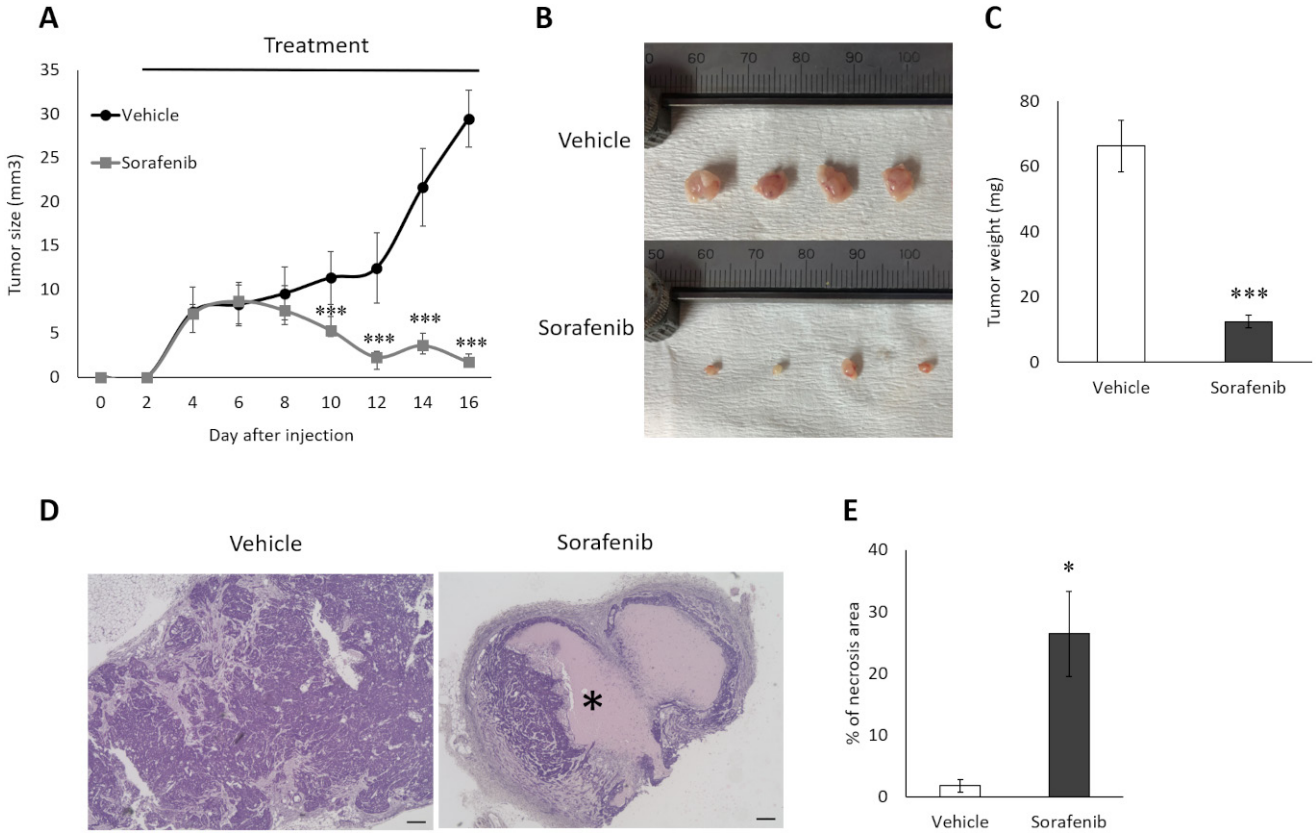

Fig. 3. Anti-tumor effect of sorafenib on canine transitional cell carcinoma (cTCC) engrafted mice. (**A**) Tumor volume of cTCC engrafted mice (n=4 each). CTCC cells were subcutaneously injected into nude mice and treated with sorafenib or vehicle for 14 days. (**B**) The images of tumors excised from tumor engrafted mice treated with sorafenib or vehicle. (**C**) Tumor weight of cTCC engrafted mice. (**D**) Histological characteristics of tumor tissues from cTCC engrafted mice. Tumor tissues were stained with hematoxylin and eosin. Asterisk indicates a necrotic area. Bars=200 μm. (**E**) The necrotic area measured by image analysis software. Each value represents the mean ± SEM. **P*<0.05, ****P*<0.001.

DISCUSSION

In this study, all cTCC cell lines expressed VEGFR-2 and PDGFR-β, and sorafenib showed growth inhibitory effects on cTCC despite differences in some parameters associated with the effects of sorafenib, such as downstream signals, cell cycle, and apoptosis. The MAPK pathway is a major stimulator of proliferation and inhibitors of apoptosis [34, 42]. In human bladder cancer, VEGF produced from immune cells in tumor microenvironment (TME) interact with VEGFR-2 on tumor cells in paracrine fashion and strongly promote tumor cell growth and angiogenesis [36]. Thus, VEGF/VEGFR-2 paracrine signal is considered to be potential therapeutic target [28]. In cTCC, the previous study performing gene expression analysis by RNA-seq revealed that VEGF was among the top upstream regulators in tumor tissue predicted to be activated, suggesting that VEGF/VEGFR-2 paracrine signal may also function in cTCC. [22]. In this study, ERK1/2 phosphorylation was not observed without VEGF treatment. Then, the growth inhibitory effect of sorafenib may be caused by suppression of other signaling pathways such as JNK, p38 and ERK5 and subsequent cell cycle arrest and apoptosis. Contrary to other cTCC cell lines, the apoptosis signal was not observed in only the LCTCC cells, although sorafenib showed an equivalent growth inhibitory effect. Considering that sorafenib induces cell death in many ways, including apoptosis, necrosis, and ferroptosis [26], other mechanisms may be involved in LCTCC cell death.

Sorafenib also demonstrated anti-tumor effects in cTCC-engrafted mice. Furthermore, vascular staining showed that sorafenib suppressed angiogenesis. The treatment dose used in *in vivo* experiments (30 mg/kg, daily) was considered effective in previous studies, including the low dose conversion to human equivalent dose, suggesting that sorafenib has therapeutic potential for cTCC [7, 20].

In a phase II trial of human bladder cancer patients, sorafenib failed to show the benefits [4]. However, this study used overall survival to judge the efficacy of sorafenib and did not take into account disease-free survival that is recommended for evaluating the efficacy of molecular targeted drugs. The author mentioned this point and pointed out effectiveness of sorafenib might not have been properly evaluated. Then, there is a rationale for clinical trials of sorafenib alone or in combination with other agents in patients with cTCC.

This study has a potential limitation that could be addressed in future studies. Subcutaneous model mice do not completely

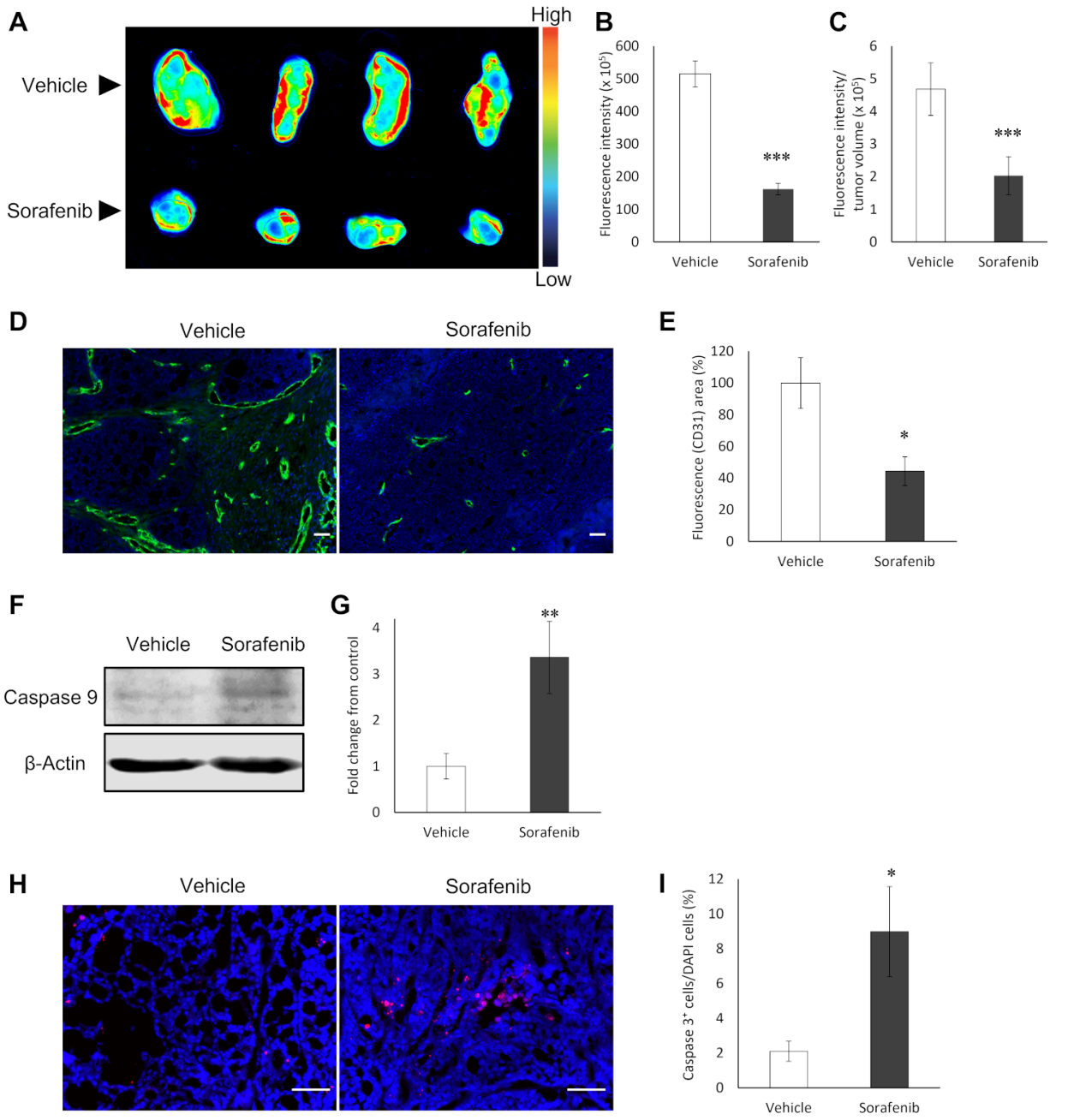

Fig. 4. The effects of sorafenib on angiogenesis and apoptosis in canine transitional cell carcinoma (cTCC) engrafted mice. (**A**) The image of vascular *in vivo* imaging of tumor tissues from cTCC engrafted mice injected with IRDye 800CW PEG Fluorescent Contrast Agent. (**B**) The fluorescence intensity in tumor tissues. (**C**) The fluorescence intensity corrected by tumor volume. (**D**) Representative examples of CD31 immunofluorescence of tumor tissues from cTCC engrafted mice. CD31 positive staining is shown in green. (**E**) The ratio of CD31 positive area. (**F**) Caspase 9 expression in tumor tissues was analyzed using western blotting. (**G**) The band densities of caspase 9 were quantified and normalized using β-actin as the corresponding control. (**H**) Representative examples of cleaved caspase 3 immunofluorescence of tumor tissues from cTCC engrafted mouse. Red fluorescence indicates cleaved caspase 3 positive cells, and blue indicates DAPI signals. Bars=50 µm (**I**) The proportion of cleaved caspase 3 positive cells. Bars=200 µm. Each value represents the mean ± SEM. **P*<0.05, ***P*<0.01 ****P*<0.001.

reflect the TME, including blood vessels, infiltrating immune cells, fibroblasts, and extracellular matrix of the actual cases with cTCC. Further studies are needed to verify the effectiveness of sorafenib using a bladder transplant model or actual clinical cases.

In conclusion, we demonstrated the anti-tumor effect of sorafenib on cTCC in both *in vitro* and *in vivo* experiments. Sorafenib inhibited tumor growth by inducing cell cycle arrest and apoptosis. Furthermore, sorafenib showed an anti-tumor effect on cTCC-engrafted mice not only by its direct effect on tumor cells but also by the indirect effect on angiogenesis in the TME. These results suggest that sorafenib is a new treatment option for cTCC.

CONFLICT OF INTEREST. The authors have nothing to disclose.

ACKNOWLEDGMENTS. We thank Dr. Y. Hoshino (Hokkaido University), Dr. K. Saeki, Dr. T. Nakagawa, and Dr. R. Nishimura (Tokyo University) for providing the canine transitional cell carcinoma cell lines. This study was supported by JSPS KAKENHI, a Grant-in-Aid for Science Research (Grant Number: 19H00968, 16H06208), and the Anicom Capital Research Grant (EVOLVE).

REFERENCES

1. Bryan, J. N., Keeler, M. R., Henry, C. J., Bryan, M. E., Hahn, A. W. and Caldwell, C. W. 2007. A population study of neutering status as a risk factor for canine prostate cancer. *Prostate* **67**: 1174–1181. [Medline] [CrossRef]
2. Chu, J. S., Ge, F. J., Zhang, B., Wang, Y., Silvestris, N., Liu, L. J., Zhao, C. H., Lin, L., Brunetti, A. E., Fu, Y. L., Wang, J., Paradiso, A. and Xu, J. M. 2013. Expression and prognostic value of VEGFR-2, PDGFR-β, and c-Met in advanced hepatocellular carcinoma. *J. Exp. Clin. Cancer Res.* **32**: 16. [Medline] [CrossRef]
3. Decker, B., Parker, H. G., Dhawan, D., Kwon, E. M., Karlins, E., Davis, B. W., Ramos-Vara, J. A., Bonney, P. L., McNiel, E. A., Knapp, D. W. and Ostrander, E. A. 2015. Homologous mutation to human BRAF V600E is common in naturally occurring canine bladder cancer-evidence for a relevant model system and urine-based diagnostic test. *Mol. Cancer Res.* **13**: 993–1002. [Medline] [CrossRef]
4. Dreicer, R., Li, H., Stein, M., DiPaola, R., Eleff, M., Roth, B. J. and Wilding, G. 2009. Phase 2 trial of sorafenib in patients with advanced urothelial cancer: a trial of the Eastern Cooperative Oncology Group. *Cancer* **115**: 4090–4095. [Medline] [CrossRef]
5. Escudier, B., Worden, F. and Kudo, M. 2019. Sorafenib: key lessons from over 10 years of experience. *Expert Rev. Anticancer Ther.* **19**: 177–189. [Medline] [CrossRef]
6. Eto, S., Saeki, K., Yoshitake, R., Yoshimoto, S., Shinada, M., Ikeda, N., Kamoto, S., Tanaka, Y., Kato, D., Maeda, S., Tsuboi, M., Chambers, J., Uchida, K., Nishimura, R. and Nakagawa, T. 2019. Anti-tumor effects of the histone deacetylase inhibitor vorinostat on canine urothelial carcinoma cells. *PLoS One* **14**: e0218382. [Medline] [CrossRef]
7. Fang, Z., Jung, K. H., Yan, H. H., Kim, S. J., Rumman, M., Park, J. H., Han, B., Lee, J. E., Kang, Y. W., Lim, J. H. and Hong, S. S. 2018. Melatonin synergizes with sorafenib to suppress pancreatic cancer via melatonin receptor and PDGFR-β/STAT3 Pathway. *Cell. Physiol. Biochem.* **47**: 1751–1768. [Medline] [CrossRef]
8. Frasca, F., Nucera, C., Pellegriti, G., Gangemi, P., Attard, M., Stella, M., Loda, M., Vella, V., Giordano, C., Trimarchi, F., Mazzon, E., Belfiore, A. and Vigneri, R. 2008. BRAF(V600E) mutation and the biology of papillary thyroid cancer. *Endocr. Relat. Cancer* **15**: 191–205. [Medline] [CrossRef]
9. Fulkerson, C. M. and Knapp, D. W. 2015. Management of transitional cell carcinoma of the urinary bladder in dogs: a review. *Vet. J.* **205**: 217–225. [Medline] [CrossRef]
10. Geschwind, J. F. H. and Chapiro, J. 2016. Sorafenib in combination with transarterial chemoembolization for the treatment of hepatocellular carcinoma. *Clin. Adv. Hematol. Oncol.* **14**: 585–587. [Medline]
11. Guida, T., Anaganti, S., Provitera, L., Gedrich, R., Sullivan, E., Wilhelm, S. M., Santoro, M. and Carlomagno, F. 2007. Sorafenib inhibits imatinib-resistant KIT and platelet-derived growth factor receptor β gatekeeper mutants. *Clin. Cancer Res.* **13**: 3363–3369. [Medline] [CrossRef]
12. Hahn, O. and Stadler, W. 2006. Sorafenib. *Curr. Opin. Oncol.* **18**: 615–621. [Medline] [CrossRef]
13. Jiang, W., Wang, D., Liu, X., Zheng, W., Wen, L., Shi, H., Zhang, H., Zhou, A., Li, C., Ma, J., Zheng, S. and Shou, J. 2021. PD-L1 and VEGFR-2 expression in synchronous metastatic renal cell carcinoma treated with targeted therapy following cytoreductive nephrectomy. *Urol. Oncol.* **39**: 78.e9–78.e16. [Medline] [CrossRef]
14. Jung, H., Bae, K., Lee, J. Y., Kim, J. H., Han, H. J., Yoon, H. Y. and Yoon, K. A. 2021. Establishment of canine transitional cell carcinoma cell lines harboring BRAF V595E mutation as a therapeutic target. *Int. J. Mol. Sci.* **22**: 9151. [Medline] [CrossRef]
15. Kim, J. H., Ahn, D. H., Moon, J. S., Han, H. J., Bae, K. and Yoon, K. A. 2021. Longitudinal assessment of B-RAF V595E levels in the peripheral cell-free tumor DNA of a 10-year-old spayed female Korean Jindo dog with unresectable metastatic urethral transitional cell carcinoma for monitoring the treatment response to a RAF inhibitor (sorafenib). *Vet. Q.* **41**: 153–162. [Medline] [CrossRef]
16. Knapp, D. W., Ramos-Vara, J. A., Moore, G. E., Dhawan, D., Bonney, P. L. and Young, K. E. 2014. Urinary bladder cancer in dogs, a naturally occurring model for cancer biology and drug development. *ILAR J.* **55**: 100–118. [Medline] [CrossRef]
17. Knapp, D. W., Ruple-Czerniak, A., Ramos-Vara, J. A., Naughton, J. F., Fulkerson, C. M. and Honkisz, S. I. 2016. A nonselective cyclooxygenase inhibitor enhances the activity of vinblastine in a naturally-occurring canine model of invasive urothelial carcinoma. *Bladder Cancer* **2**: 241–250. [Medline] [CrossRef]
18. Knapp, D. W., Henry, C. J., Widmer, W. R., Tan, K. M., Moore, G. E., Ramos-Vara, J. A., Lucroy, M. D., Greenberg, C. B., Greene, S. N., Abbo, A. H., Hanson, P. D., Alva, R. and Bonney, P. L. 2013. Randomized trial of cisplatin versus firocoxib versus cisplatin/firocoxib in dogs with transitional cell carcinoma of the urinary bladder. *J. Vet. Intern. Med.* **27**: 126–133. [Medline] [CrossRef]
19. Kopparapu, P. K., Boorjian, S. A., Robinson, B. D., Downes, M., Gudas, L. J., Mongan, N. P. and Persson, J. L. 2013. Expression of VEGF and its receptors VEGFR1/VEGFR2 is associated with invasiveness of bladder cancer. *Anticancer Res.* **33**: 2381–2390. [Medline]
20. Kuczynski, E. A., Lee, C. R., Man, S., Chen, E. and Kerbel, R. S. 2015. Effects of sorafenib dose on acquired reversible resistance and toxicity in hepatocellular carcinoma. *Cancer Res.* **75**: 2510–2519. [Medline] [CrossRef]
21. Liu, L., Zhu, D., Gao, R. and Guo, H. 2008. Expression of vascular endothelial growth factor, receptor KDR and p53 protein in transitional cell carcinoma of the bladder. *Urol. Int.* **81**: 72–76. [Medline] [CrossRef]
22. Maeda, S., Tomiyasu, H., Tsuboi, M., Inoue, A., Ishihara, G., Uchikai, T., Chambers, J. K., Uchida, K., Yonezawa, T. and Matsuki, N. 2018. Comprehensive gene expression analysis of canine invasive urothelial bladder carcinoma by RNA-Seq. *BMC Cancer* **18**: 472. [Medline] [CrossRef]
23. Marconato, L., Zini, E., Lindner, D., Suslak-Brown, L., Nelson, V. and Jeglum, A. K. 2011. Toxic effects and antitumor response of gemcitabine in combination with piroxicam treatment in dogs with transitional cell carcinoma of the urinary bladder. *J. Am. Vet. Med. Assoc.* **238**: 1004–1010. [Medline] [CrossRef]
24. Mochizuki, H., Kennedy, K., Shapiro, S. G. and Breen, M. 2015. BRAF mutations in canine cancers. *PLoS One* **10**: e0129534. [Medline] [CrossRef]
25. Mochizuki, H. and Breen, M. 2015. Comparative aspects of BRAF mutations in canine cancers. *Vet. Sci.* **2**: 231–245. [Medline] [CrossRef]

26. Nie, J., Lin, B., Zhou, M., Wu, L. and Zheng, T. 2018. Role of ferroptosis in hepatocellular carcinoma. *J. Cancer Res. Clin. Oncol.* **144**: 2329–2337. [Medline] [CrossRef]
27. Papadopoulos, N. and Lennartsson, J. 2018. The PDGF/PDGFR pathway as a drug target. *Mol. Aspects Med.* **62**: 75–88. [Medline] [CrossRef]
28. Peng, S., Zhang, Y., Peng, H., Ke, Z., Xu, L., Su, T., Tsung, A., Tohme, S., Huang, H., Zhang, Q., Lencioni, R., Zeng, Z., Peng, B., Chen, M. and Kuang, M. 2016. Intracellular autocrine VEGF signaling promotes EBDC cell proliferation, which can be inhibited by Apatinib. *Cancer Lett.* **373**: 193–202. [Medline] [CrossRef]
29. Robat, C., Burton, J., Thamm, D. and Vail, D. 2013. Retrospective evaluation of doxorubicin-piroxicam combination for the treatment of transitional cell carcinoma in dogs. *J. Small Anim. Pract.* **54**: 67–74. [Medline] [CrossRef]
30. Ross, J. S. and Fletcher, J. A. 1999. The HER-2/neu oncogene: prognostic factor, predictive factor and target for therapy. *Semin. Cancer Biol.* **9**: 125–138. [Medline] [CrossRef]
31. Scartozzi, M., Faloppi, L., Svegliati Baroni, G., Loretelli, C., Piscaglia, F., Iavarone, M., Toniutto, P., Fava, G., De Minicis, S., Mandolesi, A., Bianconi, M., Giampieri, R., Granito, A., Facchetti, F., Bitetto, D., Marinelli, S., Venerandi, L., Vavassori, S., Gemini, S., D'Errico, A., Colombo, M., Bolondi, L., Bearzi, I., Benedetti, A. and Cascinu, S. 2014. VEGF and VEGFR genotyping in the prediction of clinical outcome for HCC patients receiving sorafenib: the ALICE-1 study. *Int. J. Cancer* **135**: 1247–1256. [Medline] [CrossRef]
32. Shapiro, S. G., Raghunath, S., Williams, C., Motsinger-Reif, A. A., Cullen, J. M., Liu, T., Albertson, D., Ruvolo, M., Bergstrom Lucas, A., Jin, J., Knapp, D. W., Schiffman, J. D. and Breen, M. 2015. Canine urothelial carcinoma: genomically aberrant and comparatively relevant. *Chromosome Res.* **23**: 311–331. [Medline] [CrossRef]
33. Soria, F., Moschini, M., Haitel, A., Wirth, G. J., Karam, J. A., Wood, C. G., Rouprêt, M., Margulis, V., Karakiewicz, P. I., Briganti, A., Raman, J. D., Kammerer-Jacquet, S. F., Mathieu, R., Bensalah, K., Lotan, Y., Özsoy, M., Remzi, M., Gust, K. M. and Shariat, S. F. 2017. HER2 overexpression is associated with worse outcomes in patients with upper tract urothelial carcinoma (UTUC). *World J. Urol.* **35**: 251–259. [Medline] [CrossRef]
34. Sun, Y., Liu, W. Z., Liu, T., Feng, X., Yang, N. and Zhou, H. F. 2015. Signaling pathway of MAPK/ERK in cell proliferation, differentiation, migration, senescence and apoptosis. *J. Recept. Signal Transduct. Res.* **35**: 600–604. [Medline] [CrossRef]
35. Walters, L., Martin, O., Price, J. and Sula, M. M. 2018. Expression of receptor tyrosine kinase targets PDGFR-β, VEGFR2 and KIT in canine transitional cell carcinoma. *Vet. Comp. Oncol.* **16**: E117–E122. [Medline] [CrossRef]
36. Xia, G., Kumar, S. R., Hawes, D., Cai, J., Hassanieh, L., Groshen, S., Zhu, S., Masood, R., Quinn, D. I., Broek, D., Stein, J. P. and Gill, P. S. 2006. Expression and significance of vascular endothelial growth factor receptor 2 in bladder cancer. *J. Urol.* **175**: 1245–1252. [Medline] [CrossRef]
37. Xing, M. 2007. BRAF mutation in papillary thyroid cancer: pathogenic role, molecular bases, and clinical implications. *Endocr. Rev.* **28**: 742–762. [Medline] [CrossRef]
38. Yamaoka, T., Kusumoto, S., Ando, K., Ohba, M. and Ohmori, T. 2018. Receptor tyrosine kinase-targeted cancer therapy. *Int. J. Mol. Sci.* **19**: 1–35. [Medline] [CrossRef]
39. Yamazaki, H., Iwano, T., Otsuka, S., Kagawa, Y., Hoshino, Y., Hosoya, K., Okumura, M. and Takagi, S. 2015. SiRNA knockdown of the DEK nuclear protein mRNA enhances apoptosis and chemosensitivity of canine transitional cell carcinoma cells. *Vet. J.* **204**: 60–65. [Medline] [CrossRef]
40. Yosef, H. K., Frick, T., Hammoud, M. K., Maghnouj, A., Hahn, S., Gerwert, K. and El-Mashtoly, S. F. 2018. Exploring the efficacy and cellular uptake of sorafenib in colon cancer cells by Raman micro-spectroscopy. *Analyst (Lond.)* **143**: 6069–6078. [Medline] [CrossRef]
41. Yoshitake, R., Saeki, K., Watanabe, M., Nakaoka, N., Ong, S. M., Hanafusa, M., Choisunirachon, N., Fujita, N., Nishimura, R. and Nakagawa, T. 2017. Molecular investigation of the direct anti-tumour effects of nonsteroidal anti-inflammatory drugs in a panel of canine cancer cell lines. *Vet. J.* **221**: 38–47. [Medline] [CrossRef]
42. Yuan, L., Wang, J., Xiao, H., Wu, W., Wang, Y. and Liu, X. 2013. MAPK signaling pathways regulate mitochondrial-mediated apoptosis induced by isoorientin in human hepatoblastoma cancer cells. *Food Chem. Toxicol.* **53**: 62–68. [Medline] [CrossRef]
43. Zhang, Z., Neiva, K. G., Lingen, M. W., Ellis, L. M. and Nör, J. E. 2010. VEGF-dependent tumor angiogenesis requires inverse and reciprocal regulation of VEGFR1 and VEGFR2. *Cell Death Differ.* **17**: 499–512. [Medline] [CrossRef]
44. Zhu, Y. J., Zheng, B., Wang, H. Y. and Chen, L. 2017. New knowledge of the mechanisms of sorafenib resistance in liver cancer. *Acta Pharmacol. Sin.* **38**: 614–622. [Medline] [CrossRef]